Ionization Rates: a Comparative Study to Predict Corona Breakdown

E. Sorolla, I. Koufogiannis and M. Mattes

EPFL-STI-IEL-LEMA
Station 11, 1015 Lausanne, Switzerland.
eden.sorolla@epfl.ch

INTRODUCTION

Nowadays, the design of microwave components able to withstand high input powers without the risk of electrical breakdown to occur has become an important issue in standard technology requirements for space applications. The interest in this topic has increased by the market demand of microwave components that must deal with larger frequency ranges, smaller dimensions and higher input powers while still working properly. The establishment of these requirements leads to higher electric field densities which increase the risk of electrical breakdown occurring within microwave devices on board of satellites. Spacecraft vehicles are subject to the risk of plasma breakdown occurring either on the aperture of slot antennas or inside the satellite payloads during the launching or the re-entry phase of space missions in the earth or other planets' atmospheres.

The harsh space weather provides a big amount of free electrons in the satellites environment. Electrons can penetrate into the gaps existing between cable-connector transitions or male-female connector interfaces that are created by the unavoidable mechanical tolerances inherent to the manufacturing process. Accelerated by the RF field, the environmental electrons can collide with the molecules released by the outgassing from the walls of the boundaries of the microwave components or with those ones from the planetary atmospheric gas trapped inside the gaps. In the collision they can release other electrons placed on the external shells of the gas molecules producing a growth of the electron population if the involved energy is high enough. At the same time, the electrons tend to move away from the zones where there is a big amount of them to level out the electron population density and attain the chemical equilibrium, process that is called diffusion. Above a certain value of RF power the ionization is produced so quickly that the electrons are not able to escape fast enough from the zone where a high concentration of electrons is produced. This loss of local equilibrium between ionization and diffusion initiates a bigger ionization process, inducing a glowing emission [1] that may partially or completely damage the microwave component on board the satellites with the subsequent failure of the complete mission. This kind of discharge is called Corona breakdown and its predicted power threshold is characterized by the ionization rate and the diffusion models that are used.

In order to study the impact of different ionization rate models on the predicted Corona breakdown power threshold, a 2D Galerkin Finite Element Method (FEM) has been implemented to solve the Corona equation. Different ionization rate models found and used in literature have been studied and compared for several examples in this work.

Preliminary results show that different models predict breakdown powers that can significantly differ from each other for some devices and geometries. In this paper we focus especially on parallel-plate and coaxial geometries but the conclusions drawn from these particular cases may be applied to general cases too. It is, therefore, required to use well-established ionization rate models in the simulation tools to predict accurately the Corona breakdown threshold of microwave components as it will be shown next. Moreover, there are many technical difficulties to measure the ionization rates at very low pressures and very high effective electric fields [2,3] what limits even more the applicability of the models to the simulations.

THEORY

Corona Equation

If we define the electron population density inside a gas as $n(\vec{r},t)$, we can apply the continuity equation for the electron population assuming an arbitrarily small volume within the gas cloud. Therefore, the change of the electron population with respect to the time inside this volume is given by the flow of electrons leaving this zone in order to preserve the conservation of charge principle, what produces a current density called $\vec{J}$. However, some electrons are released from the shells of the molecules due to the ionization collisions, increasing the *change* of the electron

population density with respect to the time $(\partial n/\partial t)$ by an amount equal to the ionization rate, ν_i, times the amount of electrons per unit volume enclosed in the arbitrarily small volume: $(\nu_i n)$. Therefore, the equation that we have to deal with can be written as follows:

$$\frac{\partial n}{\partial t} = \nu_i n - \vec{\nabla} \cdot \vec{J} \ . \tag{1}$$

The electron flow through the boundaries of the considered volume is produced by the diffusion process, and it can be proved that the current density due to diffusion is given by [4]

$$\vec{J} = -\vec{\nabla} \cdot (Dn) , \tag{2}$$

where D is the diffusion coefficient. For this work we have chosen the diffusion model given by [5], where D is expressed for air as:

$$D = 1.6 \cdot 10^6 / p \tag{3}$$

in the CGS system, preserving the form of the diffusion coefficient as given by the reference above. In this metric system of physical units, p is the pressure given in Torr (mmHg) and distances are in cm. Thus, the Corona equation can be written as follows:

$$\frac{\partial n}{\partial t} = \nu_i n + D\nabla^2 n \ . \tag{4}$$

The general criterion to consider the appearance of Corona breakdown is found calculating the power that yields the chemical equilibrium in the electron population density, i.e. when $\partial n/\partial t = 0$. Under this condition a slightly higher input power will induce an ionization rate whose effects will overcome the losses by diffusion, and the electron population will grow exponentially triggering the Corona discharge onset.

To describe the ionization process we have to take into consideration that the electrons are accelerated by the RF field and they may either experience many collisions before they reach enough energy to ionize a gas molecule or be accelerated forth and back several times before colliding against a neutral molecule. The average number of collisions per unit time is called the collision rate, ν_c, which depends on the gas pressure. It is observed that there is a pressure for which the efficiency in the gain of energy of the electrons, driven by the microwave field, is optimal. That pressure is near the one for which the collision rate equals the microwave frequency ω. Many authors have measured the collision rate for air, agreeing most of them with the expression [7,8]:

$$\nu_c = 5.3 \cdot 10^9 \, p \ . \tag{5}$$

Ionization Rate Models

Since the ionization rate models are based on DC experiments the concept of the effective electric field is used to take into account the efficiency in the collisions between electrons and neutrals. The effective electric field can be considered as the DC equivalent of the RF peak electric field. The relation is given by [4]:

$$E_e = \frac{E_{rms}}{\sqrt{1 + \left(\frac{\omega}{\nu_c}\right)^2}} , \tag{6}$$

where E_{rms} is the time-average RF electric field. From Eq. (6) it follows directly that for DC fields E_e equals to E_{rms}.
Several models for the ionization rate can be found in the literature. In this work we have used the models extracted from [6, 9, 10], which are based on semi-empirical arguments, to calculate the predicted Corona breakdown threshold for different waveguides. We have referred to each model according to the name of the first author of the aforementioned references.

In Fig. 1 the different ionization rates, that are going to be compared along this paper, are shown in a log-log plot for better comparison within its range of validity: $E_e/p \in [30,100]$ [6,9]. Noticeable differences between the values of the ionization rates provided by the models can be observed. We will study how these discrepancies result in different predicted breakdown electric fields and, consequently, in different Corona breakdown power thresholds.

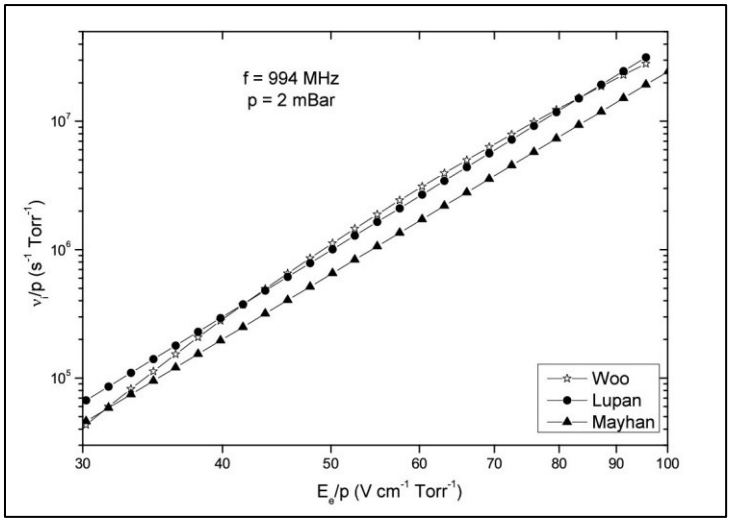

Fig. 1. Ionization rate models.

At this point a specific remark must be done about Mayhan's ionization rate model since it is developed in the framework of re-entry vehicles in a high temperature environment as it occurs in the ionosphere. A low temperature has been considered in this paper (~300K) providing lower values of the ionization rate than the ones of the other models, overall for big values of E_e/p.

Test Cases

The parallel-plate waveguide as well as the coaxial one have been chosen as representative examples to show the Corona breakdown predictions provided by the different ionization rate models. For both devices it suffices to assume a TEM field distribution between the electrodes subject to a voltage *V(t)*.

Parallel-plate Waveguide

In the case of the parallel plates separated by a distance *d* (see Fig. 2) the electric field is constant and equal to $V(t)/d$, i.e. the ionization rate is also constant in the region between the plates. Therefore, we can solve Eq. (4) analytically because all the coefficients are constant.

Due to the symmetry of the problem we can consider only the variation of the electron density along the *z* axis (see Fig. **2**) assuming an initially homogeneous distribution of the electron density between the plates. Thus, we can apply the separation of variables technique for 1D. Regarding the boundary conditions, we can expect that the electrons will quickly recombine with the atoms of the metal when reaching any plate, so that the electron density can be considered zero on the metals. This can be expressed by the following boundary conditions:

$$n\big|_{z=0} = n\big|_{z=d} = 0 \quad \forall (x, y, t) . \tag{7}$$

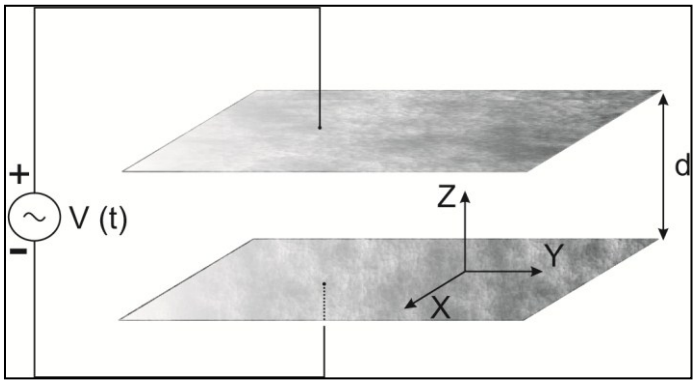

Fig. 2. Parallel-plate waveguide sketch.

Therefore, we find the solution to be

$$n(z,t) \propto \sin\left(\sqrt{\frac{\gamma}{D}}z\right) e^{(\nu_i-\gamma)t}, \tag{8}$$

where the parameter γ must read $\gamma = \left(\frac{m\pi}{d}\right)^2 D$, in order to verify the boundary conditions, and m is a non-zero integer number. As the ionization rate depends on the electric field and the pressure, and the diffusion coefficient does on the latter one, too, there will exist, at a given pressure, a breakdown electric field E_B, corresponding to $m = 1$, which establishes the breakdown condition as

$$\nu_i(p, E_B) - \gamma(p) = 0 \tag{9}$$

above which the Corona discharge will occur. Since (9) constitutes a non-linear equation, a bisection root search algorithm has been applied to compute the breakdown electric field, E_B of (9) for each pressure, and the Paschen curve is obtained [11]. The bisection algorithm was used in all the simulations along this work since, although its convergence is slow, it is always ensured.

To calculate the Corona breakdown power from the breakdown electric field, we define the power per unit length as

$$\frac{dP_B}{dy} = \frac{d}{240\pi}\left|E_B\right|^2, \tag{10}$$

since the parallel-plate is supposed to have an infinite width.

Coaxial Waveguide

The electric field within a coaxial waveguide is not constant and, consequently, the ionization rate coefficient either. Thus, to predict the Corona breakdown threshold, a 2D Galerkin FEM code has been implemented using the electric field provided by the analytical solution of the coaxial waveguide excited by the TEM mode:

$$\vec{E} = \frac{\sqrt{\eta_0 P}}{\rho\sqrt{\ln(b/a)}}\hat{\rho}, \tag{11}$$

where P is the input power, b and a are the outer and inner radius of the coaxial, respectively, and ρ is the radial component in the cylindrical coordinates system (see Fig**. 3**).

The mesh was created with the free software package Gmsh [12] and the value of the electric field at each node of the triangular mesh was calculated using (11), approximating the electric field within the finite elements by linear interpolation. The power that yields to the first zero of the determinant of the discretized Corona equation was searched for different pressures using, again, the bisection algorithm, yielding the Paschen curve.

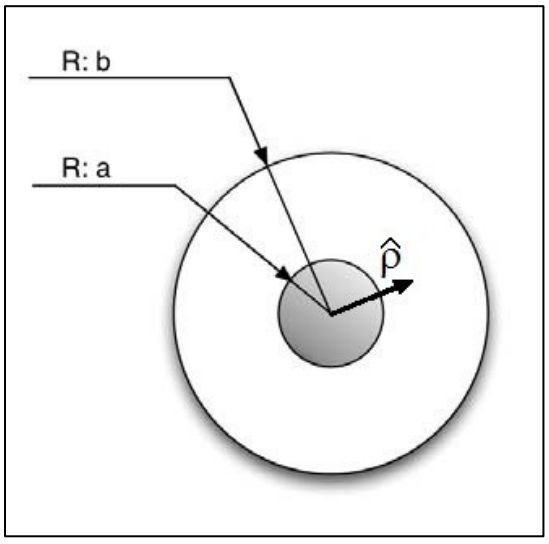

Fig. 3. Coaxial cross-section sketch.

RESULTS

Parallel-plate Results

In this section, the Paschen curve of the breakdown power obtained with different ionization rate models for the parallel-plate waveguide is going to be presented and the results to be compared.

In Fig. 4 the results obtained for a waveguide of dimensions d=4.74 cm, at the frequency f=0.994 GHz are shown. The experimental results obtained by MacDonald [13] have also been added for comparison. Looking at the Fig. 1 it can be noticed that, the higher the ionization rate, the lower the predicted breakdown threshold, as expected. The Fig. 4 shows that the minimum of the Paschen curve obtained with the Woo model and with the Mayhan one differ up to 20%. Notice that the Paschen curves obtained by the different models cross each other in some points as the ionization rates do (see Fig. 1).

Coaxial Results

The predicted values of the Corona breakdown power for a coaxial waveguide obtained by the different ionization rate models together with the measurements presented in [14] are shown in Fig. 5. In this case it can be noticed that the discrepancies between the minimum of the Paschen curve obtained by the Lupan model and the one obtained by the Woo model reach differences up to 30%. Nevertheless, in some parts of the plot differences of more than 3dB between the predictions obtained by the Lupan model and the Woo one can be observed. Notice that the Paschen curves cross each other, too, in this case, that the Woo model predicts higher breakdown powers at low pressures and that the Mayhan model predicts higher values above 5 mBar. This behaviour can be understood as in Fig. 1 the ionization rates of different models cross as well for certain values of the ratio of effective electric field over pressure.

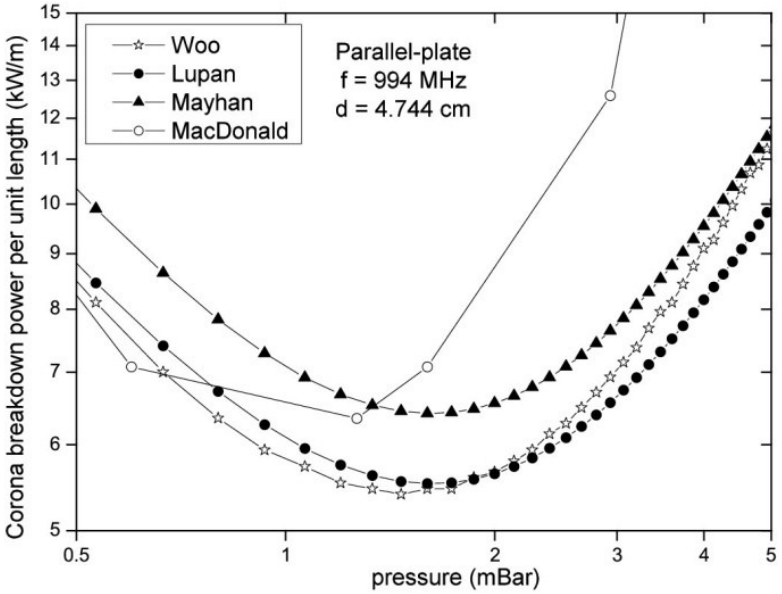

Fig. 4. Paschen curve for air of a parallel-plate waveguide together with MacDonald measurements.

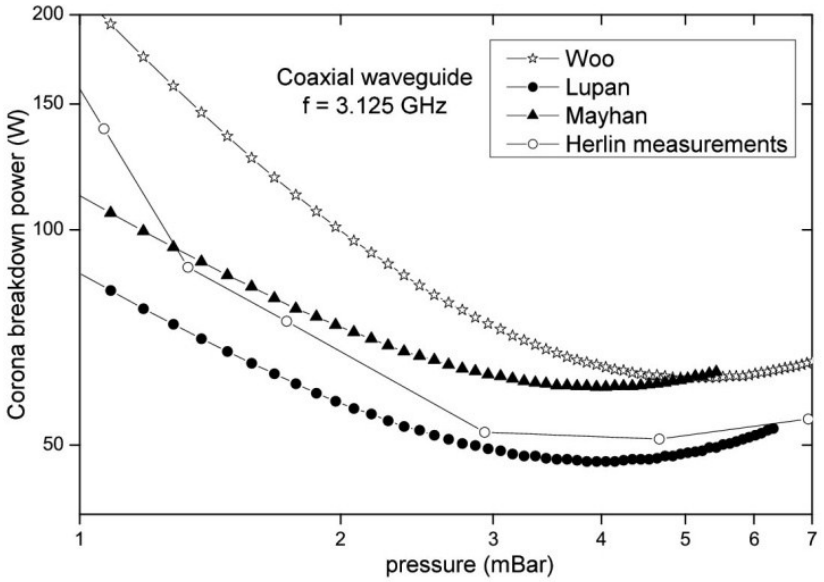

Fig. 5. Paschen curve for air of a coaxial waveguide of dimensions a = 0.318mm, b = 4.77mm, together with measurements [14].

CONCLUSIONS

The breakdown power threshold of a microwave device for space applications is fundamental to ensure the good performance of satellites and space vehicles. This factor provides an important constraint in the design of electron devices on board of satellites. Three different available models of the ionization rate for low-pressure microwave discharges are studied in this paper. Noticeable discrepancies in the predicted breakdown power obtained by the different models have been observed.

Moreover, for most of the models the ionization rate is only valid for a relatively small range of values of the ratio of effective electric field over pressure. This fact limits the values of the RF frequency and gap distance for which the simulations of the Corona breakdown power threshold can be done without leaving the range of validity of the models. It would be interesting to propose experimental setups to measure the ionization rate dealing with lower pressures and higher effective electric fields than considered so far. This will increase the validity range of the models and thus, a larger range of waveguide dimensions, frequencies and pressures could be used to simulate the Paschen curve all along the range of the ratio effective electric field over pressure.

ACKNOWLEDGMENTS

This work has been supported by the Swiss National Science Foundation (SNF) under the project *Modelling microwave-electron interaction in the LHC beam pipe* (SNF contract no. 200021_129661).

REFERENCES

[1] Yu. S. Akishev, M. E. Grushin, A. A. Deryugin, A. P. Napartovich, M. V. Pan'kin and N. I. Trushkin, "Self-oscillations of a positive corona in nitrogen", J. *Phys. D: Appl. Phys.* **32**, 1999.

[2] J. Dutton, F. M. Harris and F. Llewellyn Jones, "The determination of Attachment and Ionization Coefficients in Air", *Proc. Phys. Soc.*, Vol. 81, 1963.

[3] A. G. Sobol and G. A. Sobol, "Concerning the problem of measuring the ionization rate in a plasma"*, Radiofizika*, Vol. 17, No. 7, 1974.

[4] E. Nasser, *Fundamentals of gaseous ionization and plasma electronics*. John Wiley & Sons Inc. 1971.

[5] D. Kelly and H. Margenau, "High-Frequency Breakdown of Air", *J. Appl. Phys.* **31**, No. 9, 1960.

[6] W. Woo and J. S. DeGroot, "Microwave absorption and plasma heating due to microwave breakdown in the atmosphere", *Phys. Fluids*, **27**, No. 2, 1984.

[7] R. A. Nielsen and N. E. Bradbury, "Electron and Negative Ion Mobilities in Oxygen, Air, Nitrous Oxide and Ammonia", *Phys. Rev.* **51**, 69, 1937.

[8] H. Ryzko, "Drift velocity of electrons and ions in dry and humid air and in water vapour", *Proc. Phys. Soc.* **85**, 1283, 1965.

[9] Yu. A. Lupan, A. A. Krasutskii and S. V. Zakrevskii, "Microwave breakdown field in air", *Zh. Tekh. Fiz.* **48**, 1978.

[10] J. T. Mayhan, R. L. Fante, R. O'Keefe, R. Elkin, J. Klugerman and J. Yos, "Comparison of Various Microwave Breakdown Prediction Models", *J. Appl. Phys.* **42**, No. 13, 1971.

[11] F. Paschen, "Über die zum Funkenübergang in Luft, Wasserstoff und Kohlensäure bei verschiedenen Drucken erforderliche Potentialdifferenz", *Annalen der Physik***, 273**, No. 5, 1889.

[12] http://www.geuz.org/gmsh/

[13] A. D. MacDonald, *Microwave Breakdown in Gases*, John Wiley & Sons, Inc., 1966.

[14] M. A. Herlin and S. C. Brown, "Electrical Breakdown of a Gas between Coaxial Cylinders at Microwave Frequencies", *Physical Review*, **74**, No. 8, 1948.